Nuclear Instruments and Methods 0 (1982) , V. 203 , N 1-3 , p 523-526.
North-Holland Publishing Company

DISORDER DEPENDENCE OF ION IMPLANTED GaAs ON THE TYPE OF ION

I.S. TASHLYKOV

Institute of Applied Physics, Byelorussian State University, 220080 Minsk, U.S.S.R.

Received 5 August 1981 and in revised form 22 December 1981

Channeling experiments with 1.0 MeV He$^+$ ions have been carried out to study lattice damage of (111) GaAs crystals after 60 and 110 keV aluminum and phosphorus implantation. The implantation and the channeling measurements have been performed in situ at 42 K and at room temperature (RT). Implant doses ranged from 2.8×10^{12} to 8×10^{16} ions/cm^2.

We have observed large differences in the level of the measured damage for Al$^+$ and P$^+$ implantations into GaAs at RT within a dose range 10^{13}–10^{15} ions/cm^2. The chemical nature of the interaction between Al$^+$ and P$^+$ and GaAs is different. Consequently, it is perposed that the effect can be explained by different types of defect formation.

1. Introduction

Peculiarities of radiation damage, spatial distributions of implanted atoms and structural transformations occurring during ion implantation into solids are problems of pure and applied fields of science. Consequently it is a matter of interest to study radiation damage of GaAs implanted by Al$^+$ and P$^+$ ions.

Previous experiments [1–4] have shown the complex nature of radiation disorder of GaAs crystals in case of Al$^+$ and P$^+$ implantation. An interpretation of these experimental observations if often inconsistent. Considerable disorder of the GaAs implanted at RT with Al is explained by a non-uniform distribution of aluminum [3]. In the same work the changes of signal (combination light scattering technique), at high temperature of implantation is accounted for by a rising rate of the target sputtering. In contrast to this conclusion, authors of ref. 2 have observed, using the electron-induced luminescence method, that the width of the layer which luminescenced in the short wave region grew to 0.4 μm ($\bar{R}_p = 0.44$ μm and $\Delta\bar{R}_p = 0.028$ μm for $E_{Al} = 50$ keV [5]) at high temperature implantation.

In the present work we report new observation of the implantation behaviour of GaAs, using Al and P implants with energy 60 and 110 keV. The production of damage as a function of the ion dose both at low and room temperatures has been determined.

2. Experimental

GaAs single crystals of (111) orientation were implanted by Al$^+$ and P$^+$ ions at energies 60 and 110 keV. Implantation was carried out along nonchanneling direction both at 42 K and room temperature, using a magnetically analyzed and swept ion beam in a vacuum system with base pressure in the 10^{-7}-Torr range. Implantation doses, ranging from 2.8×10^{12} to 8×10^{16} ions/cm^2 were obtained. The average beam intensities were 70–160 nA/cm^2 at 60 keV and 20–70 nA/cm^2 at 110 keV. The damage-dose behaviour of ion bombarded GaAs was measured by the channeling technique using in situ measurements.

For both the 42 K and 300 K bombardments the sample was surrounded by a 30 K cold shield to minimise any surface contamination during the experiment.

Energies of backscattered ions were measured using a surface barrier detector at 150° scattering angle. The energy resolution was 15 keV at fwhm. Radiation damage was calculated using an iterative technique based upon a linear dechanneling approximation.

3. Results

In fig. 1 the backscattering spectra are shown for Al$^+$ and P$^+$ implanted GaAs crystals. Curves 3 and 4 show the RBS spectra from crystals implanted by Al$^+$ and P$^+$ at 42 K, respectively. The curves indicate that at low temperature Al$^+$ and P$^+$ implantations result in similar level of radiation damage. Also the position and fwhm of the damage peak in the case of low and moderate doses of Al$^+$ and P$^+$ implantations into GaAs at 42 K are comparable.

The picture is different for RT irradiation. Curve 5 shows the backscattering spectrum from GaAs, implanted at RT by 1.4×10^{15} Al$^+$/cm^2 and curve 6 shows a similar spectrum for 1.4×10^{14} p$^+$/cm^2 irradiation of GaAs. Despite the fact that phosphorus implantation is one order of magnitude less than that of Al, the peak of the damage caused by Al$^+$ irradiation is consid-

0167-5087/82/0000-0000/$02.75 © 1982 North-Holland

erably less than that due to P^+ irradiation.

At high fluences ($D \geq 4 \times 10^{15}$ ions/cm^2) of implants when amorphisation has been achieved the aligned spectra from both Al^+ and P^+ implanted GaAs crystals are again very similar (curves 7 and 8). However, we note, that to amorphise the GaAs crystals by Al^+ implantation approximately one order of magnitude higher fluxes (compared to P^+) have to be used.

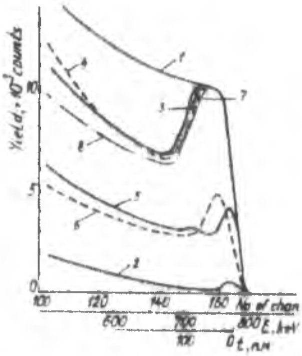

Fig. 1. Backscattering spectra of GaAs using 1.0 MeV He^+ for random – 1 and (111) channeling before implantation – 2 and after implantation at 42 K 1.4×10^{14} Al^+/cm^2 – 3; 1.35×10^{14} P^+/cm^2 – 4; at room temperature 1.4×10^{15} Al^+ – 5; 1.4×10^{14} P^+/cm^2 – 6; 8.1×10^{15} Al^+/cm^2 – 7; 4.1×10^{15} P^+/cm^2 – 8.

Damage versus dose curves are shown in fig. 2. At low temperature, when migration processes are frozen, the dynamics of damage accumulation seems to be similar for both Al^+ and P^+ irradiation (curves 1 and 2). We note, that the amount of damage resulting from Al^+ implantation is consistently lower.

At RT there are essential differences in the damage dose dependence observed for Al^+ and P^+ implantations into GaAs (curves 3 and 4 in fig. 2). These curves have three distinct regions, each with a different slope.

Fig. 3 shows defect distribution profiles in GaAs crystals implanted by 110 keV Al^+ and P^+ ions. A profile of deposited energy in P^+ radiated GaAs [6] is shown for comparison. The energy deposition of Al^+ in GaAs is distributed ~ 10 nm deeper than that for P^+ ions [6]. The energy scale of the backscattered He^+ has been converted into a depth scale using conventional energy-loss parameters [8].

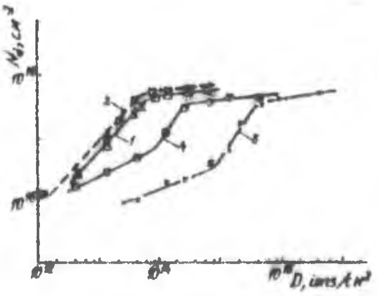

Fig. 2. The dose dependence of the lattice disorder produced in GaAs by 60 keV Al and P implantations at 42 K – 1 and 2, and room temperature – 3 and 4, respectively.

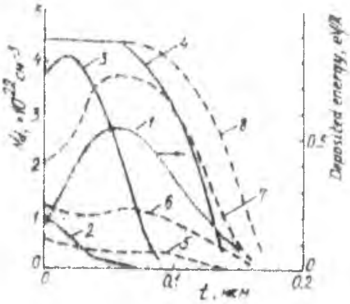

Fig. 3. Defect distribution profiles in 110 keV ion implanted at room temperature GaAs: 2.8×10^{14} Al^+/cm^2 – 2, 9.0×10^{14} Al^+/cm^2 – 3; 1.8×10^{15} Al^+/cm^2 – 4; 2.1×10^{13} P^+/cm^2 – 5; 5.3×10^{13} P^+/cm^2 – 6, 1.4×10^{14} P^+/cm^2 – 7; 3.5×10^{14} P^+/cm^2 – 8. A theoretical profile of deposited energy in P^+ radiated GaAs – 1.

4. Discussion

The RBS in conjunction [illegible] measurements have indicated that [illegible] K) Al^+ and P^+ implantation into GaAs [illegible] similar picture of the damage in the implanted crystals, curves 3 and 4 in fig. 1. For both sorts of ions implanted at low temperature in GaAs the build up of damage with dose is initially linear and the constant of proportionality is about unity, curves 1 and 2 in fig. 2. Eventually, saturation occurs and the saturation level is reached at doses of approximately 5×10^{13} P^+/cm^2 and 6×10^{13} Al^+/cm^2. The thickness of amorphous layer grows slowly with dose but the number of defects produced by Al^+ in GaAs is always less than that for P^+ ions.

Several possible reasons for this behaviour can be suggested. The effect is possibly associated with the lower fraction (0.55 compared with 0.59) of the total energy deposited into nuclear recoils by Al^+ implantation. In addition, the rest of the total released energy is bigger in the case of Al implants. Consequently, if at 42 K annealing processes during implantation exist, they may occur in more active form also in Al^+ radiated GaAs crystals.

As mentioned in section 3, the picture differs for room temperature implantation. Curves 5 and 6 in fig. 1 discussed above demonstrate this conclusion. We can add that the peak of the damage caused by Al^+ irradiation is considerable less than that due to P^+ implantation. A characteristic feature of Al^+ implantation is also the smaller depth of the damage peak position (compared with P^+ implantation and theoretical prediction [5,6]). This fact is reflected in fig. 3 as well.

As a result, there are essential differences in the damage dose dependence observed for RT Al^+ and P^+ implantations into GaAs (curves 3 and 4 in fig. 2). These curves have three distinct regions each with different slope. The first region (doses up to $\sim 1 \times 10^{14}$ P^+/cm^2 and $\sim 1 \times 10^{15}$ Al^+/cm^2) can be considered as a stage of defect accumulation. The slower rate of rise of the curve of damage with dose compared with the curves obtained at the low temperature experiment (curves 1 and 2 in fig. 2), is considered to be due to annealing of the damage, produced in GaAs both by Al^+ and P^+ implantation and by the 1 MeV helium beam used subsequently for analysis.

Similar stages of defect accumulation were observed in Si, implanted at RT with B^+ and N^+ using secondary-emission technique [7] and in GaP, which was implanted at RT with Te^+ ions (RBS measurements) [9]. The authors of both papers consider that at this stage processes of simple interaction of radiation defects (plus impurities) and the creation of stable complexes in implanted layers take place.

Our observations are in good agreement with such interpretations of experimental results. We can add, that the chemical nature of the interaction between Al and P atoms and GaAs (the atoms create chemical bonds with As and Ga atoms respectively) is probably responsible for essential differences in the level of radiation damage at that stage in the dose range up to $\sim 1 \times 10^{15}$ ions/cm^2. It is known that lattice constants are quite different for GaAs ($a_0 = 5.6532$ Å) and GaP ($a_0 = 5.4512$ Å) and almost the same for GaAs and AlAs. This means that lower energy migration processes would take place in Al^+ implanted rather than in P^+ implanted GaAs. The annealing effect therefore will be bigger in GaAs radiated by Al^+ ions. On the other hand different defect mobilities may lead to the formation of different types of secondary stable complexes. Our results confirm such assumptions. For example, in spite of the smaller peak of the damage caused by Al^+ irradiation (curve 5 in fig. 1) the dechanneling rate is even higher than that observed for P^+ implantations (curve 6).

Recent publications indicate the possibility of using a channeling technique (by mean of measuring dechanneling rate at different energy of analysed ions) to estimate types of defects in implanted crystals [10,11]. At present we are planning to apply this technique to analyse types of damage in Al^+ and P^+ radiated GaAs.

The first region in fig. 2 is followed by a stage of damage transformation, the onset of which is at $\sim 10^{14}$ P^+/cm^2 and $\sim 10^{15}$ Al^+/cm^2. The rate of increase of damage with dose becomes greater at the second stage, as shown in fig. 2, until a saturation level is reached. The implanted layer can thus be considered to be in a random or amorphous condition to a depth corresponding to the projected range plus a range of spread (curves 7 and 8 in fig. 1). The damage transformation takes place at damage levels of ~ 20 and ~ 10 percent total disorder in P^+ and Al^+ implanted GaAs, respectively. These levels agree qualitatively with the estimates of previous investigations [7,9,12].

The final region is a slow increase in amount of damage. In accordance with the changes in the RBS spectra this is considered to be due to the increase of the damage layer thickness. This means that the effect of the surface sputtering plays negligible role for Al^+ and P^+ ion doses up to 8×10^{16} cm^{-2}.

The energy of the ions was increased to 110 keV in order to restrict the surface influence of GaAs damage dependence on ion sort of implants. But in the experiments with 110 keV Al^+ and P^+ implantations into GaAs, differences in the level of damage have been estimated to be even bigger than for 60 keV ions. Data, presented in fig. 3, illustrate this behaviour. One may compare the experimental and theoretical damage profiles in Al^+ and P^+ implanted GaAs crystals. The experimental defect profile in 1.4×10^{14} P^+/cm^2 implanted GaAs is consistent with the calculated mean of the damage depth, while for low doses the concentration of defects at the surface is higher, than, or approaches, the concentration of N_d at the expected depth of the maximum position of the deposited energy distribution. Formation of the two damage peaks (the "interior" at a depth $\bar{R}_p$ and on the "surface") is a known effect in implanted semiconductors [7,13,14]. We have previously discussed [4] high concentration of radiation defects localized on the surface at the implanted at $T \geq 150$°C by P^+ GaAs crystals. In the case of Al^+ implantation into GaAs only one the "surface" peak of damage is usually formed. The depth distribution of the damage profiles in Al^+ implanted at RT GaAs crystals can be compared with theoretical prediction only for large doses when the amorphisation of the surface layer takes place (curve 4 on fig. 3). For low and moderate dose ranges (curves 2 and 3 on fig. 3), the radiation defects are concentrated at the crystal surface within a layer thickness which is a factor of 1[illegible] predicted mean of the damage depth.

5. Conclusions

In this paper we have studied lattice damage caused by ion implantation at low (42 K) and room temperatures in GaAs using Al and P ions up to 110 keV. In particular, the dependence of disorder on implanted ion dose and depth distribution of damage have been investigated. For both sorts of ions implanted at low temperature, the build up of damage with dose is linear with the constant of proportionality close to unity until an amorphisation of the implanted layer is reached at a dose of approximately 5×10^{13} P^+/cm^2 and 6×10^{13} Al^+/cm^2.

The increase of damage with ion dose in GaAs implanted at RT exibits three linear regions: a) a slow build up of damage to approximately 20 and 10 percent of saturation level at 1×10^{14} P^+/cm^2 and 1×10^{15} Al^+/cm^2, respectively; b) a faster increase of damage to the saturation level of disorder at a dose of approximately 3×10^{14} P^+/cm^2 and 4×10^{15} Al^+/cm^2; c) a very slow increase in the number of defects due to enlargement of the damaged layer thickness.

Large differences in the level of measured disorder (up to one order of magnitude) have been observed for Al^+ and P^+ implantations into GaAs at RT within the dose range 10^{13}-10^{15} ions/cm^2. This effect indicates that the chemical nature of the interaction between Al and P atoms and GaAs substrate is different and plays an important role in limitation of migration processes in the implanted layers.

In Al^+ implanted at RT into GaAs, radiation defects [illegible] more mobile than in P^+ implanted crystals. There[illegible]urface" and the "interior" damage peaks exist [illegible]ted crystals while in gaAs, implanted [illegible]e" peak is formed.

The author [illegible] express his thanks to Dr. J.A. Davies from CRNL and Dr. [illegible] from McMaster University for many critical and helpful discussions of the experimental results, and to Mr. R. Newcomb for useful assistance.

The experimental part of this investigation has been done at McMaster University under the General Exchange Agreement between the USSR and Canada. We express our acknowledgments to the SSHRC of Canada for providing of suitable conditions to do this research.

References

[1] L.H. Skolnik, W.G. Spitzer, A. Kahan and R.G. Hunsperger, J. of Appl. Phys. 42 (1971) 5223.

[2] O.N. Kuznetsov, L.V. Lezheiko, E.V. Lubopytova and L.N. Safronov, Fisika and Tekhnika Poluprovodnikov 11 (1977) 1449.

[3] I.I. Novak, V.V. Baptizmanski, N.S. Smirnova and A.V. Suvorov, Fisika Tvjordogo Tela 20 (1978) 2134.

[4] I.S. Tashlykov, Nucl. Instr. and Meth. 170 (1980) 403.

[5] A.F. Burenkov, F.F. Komarov, M.A. Kumakhov and M.M. Tjomkin, Tables of the Ion Implanted Spatial Distribution Parameters (Byelorussian State University's Publishing House, Minsk, 1980).

[6] K.B. Winterbon, Ion Implantation Range and Energy Deposition Distributions, vol. 2: Low Incident Ion Energy (IFI/Plenum, New York, 1975).

[7] I.A. Abrojan, A.I. Titov and A.V. Khlebalkin, Fisika and Tekhnika Poluprovodnikov 13 (1979) 227.

[8] Ion Beam Handbook for Materials Analysis, ed. J.W. Mayer and E. Rimini (Academic Press, New York, 1977).

[9] G. Carter, W.A. Grant, J.D. Haskell and G.A. Stephens, Rad. Effects 6 (1970) 277.

[10] S.T. Picraux, E. Rimini, G. Foti and S.U. Campisano, Phys. Rev. B 18 (1978) 2078.

[11] G. Götz, B. Gruska and H. Hedler, FSU Jena, Forschungsergebnisse No. 42 (N) (1978) 1.

[12] D.A. Thompson and R.S. Walker, Rad. Effects 30 (1976) 37.

[13] S.I. Romanov and L.S. Smirnov, Fisika and Tekhnika Poluprovodnikov 6 (1972) 1631.

[14] D.K. Sadana and G.R. Booker, Rad. Effects 42 (1979) 35.